Available online at www.sciencedirect.com
ScienceDirect
Journal of Nuclear Materials 375 (2008) 252–258
journal of nuclear materials
www.elsevier.com/locate/jnucmat

Modelling of steady state erosion of CFC actively water-cooled mock-up for the ITER divertor

O.V. Ogorodnikova *

Département de Recherches sur la Fusion Contrôlée, Association Euratom-CEA, CEA-Cadarache, F-13108 Saint Paul Lez Durance cedex, France

Received 30 January 2007

Abstract

Calculations of the physical and chemical erosion of CFC (carbon fibre composite) monoblocks as outer vertical target of the ITER divertor during normal operation regimes have been done. Off-normal events and ELM's are not considered here. For a set of components under thermal and particles loads at glancing incident angle, variations in the material properties and/or assembly of defects could result in different erosion of actively-cooled components and, thus, in temperature instabilities. Operation regimes where the temperature instability takes place are investigated. It is shown that the temperature and erosion instabilities, probably, are not a critical point for the present design of ITER vertical target if a realistic variation of material properties is assumed, namely, the difference in the thermal conductivities of the neighbouring monoblocks is 20% and the maximum allowable size of a defect between CFC armour and cooling tube is +/−90° in circumferential direction from the apex.

1. Introduction

Plasma–surface interaction will be one of the areas determining the success of ITER. The interaction of the plasma with a material in ITER will have significant impact on both the plasma performance and the lifetime of the material. The plasma-facing component should have low erosion rate, resistance to the neutron irradiation, low hydrogen isotope inventory and permeation and high heat removal efficiency, i.e. high thermal conductivity. In the ITER divertor the selection of the armour material is mainly based on the erosion lifetime assessment [1]. At the present, CFC monoblock of 50 mm of total thickness with water cooled CuCrZr tubes is a reference design for ITER high heat flux divertor area since these materials have high thermal conductivities and the monoblock is resistant to the thermofatigue stress failure. It was shown in [2] that CFC monoblock can sustain up to 20 MW/m^2 of the power load at normal incidence. Therefore, CFC has been proposed to be situated in the future fusion device ITER in a position with maximum power and particles loads, namely as outer vertical target. In this position, CFC can have high erosion and a significant risk of failure. Due to local variations of the thermal properties of different components, presence of defects and asymmetry of thermal and particle loads at glancing angle (higher load on the edge of the component), the temperature and, consequently, the erosion of neighbouring components could be different. The difference in the surface temperature distributions or in erosion profiles of two neighbouring components one can call temperature or the erosion instability, respectively. The purpose of this paper is to investigate if the difference in erosion of two neighbouring monoblocks will be increased with plasma discharges and results in an unacceptable erosion of one of the components in normal operation regimes for ITER or this erosion/temperature instability is not critical. Off-normal events (transient, disruptions, etc.) and ELMs (edge localized modes) are not considered here.

2. Input parameters

The loading parameter window for the divertor region is:

* Tel.: +33 4 42 25 3377.
E-mail address: igra32@rambler.ru

0022-3115/$ - see front matter © 2008 Elsevier B.V. All rights reserved.
doi:10.1016/j.jnucmat.2008.01.010

Plasma temperature, T_{pl}: 1–20 eV
Ion flux, I_0: 5×10^{22}–5×10^{24} m^{-2} s^{-1}
Power density, P: 1–20 MW/m^2.
The pulse duration in ITER will be higher than 400 s.

The plasma parameters near the outer vertical target, namely, power density, particle flux and plasma temperature have been calculated by B2-EIRENE [3]. According to the code B2-EIRENE, the total power load for the normal operation of ITER on the outer vertical target consists of about 30% due to irradiation from the plasma and about 70% due to particles heating. One possible case with peak power load of 4 MW/m^2 on the outer vertical target is shown in Fig. 1. The correlation of the power load with plasma temperature and deuterium particle flux is also shown. The distance $x = 0$ corresponds to the location of the separatrix. The peak heat flux occurs close to the separatrix. An increase of the power load results to the shift of the maximum of power, temperature and particle distributions to the separatrix.

The particles will impinge the target with a broad distribution of glancing angle. In the present calculations the glancing angle is taking as $\alpha = 3°$. This will result in high heat and particle fluxes on the edges of components.

Erosion of divertor components during repeated pulses and distribution of eroded material are critical issues for the performance of ITER. The erosion of the outer vertical target is defined mainly by two processes: sputtering by incident particles and thermal erosion. At temperatures below 2000 °C the contribution of the physical and chemical sputtering of carbon based materials to the total erosion is dominant compared with thermal erosion (evaporation and brittle destruction). Since the surface temperatures during normal operation regime do not reach the threshold for evaporation and brittle destruction, only the erosion due to physical sputtering and chemical erosion is considered here. Off-normal events and ELM's have not been taken into account. The calculations of the physical and chemical erosions have been done using the subroutine 'Erosion' developed inside a commercial and certificate finite element code ANSYS [4,5]. This subroutine includes physical sputtering, chemical erosion and sublimation of plasma-facing mock-ups under high heat and particle loads and allows to calculate temperature and erosion profiles for inclined particle incidence taking into account the shadowing effect. The cooling of component by radiation and by cooling water is also taking into account.

Physical sputtering yield has been calculated for the Maxwellian distribution of incident deuterium ions with average energy of 6.5 T_e [6–8] instead of usually assumed energy of 3 T_e [9,10]. Fig. 2 shows the physical sputtering yields for both Maxwellian distributions with energy of incident ions of 3 T_e [9] and energy of 6.5 T_e [7]. The real energy of impinging particles of 6.5 T_e increases the sputtering yield, especially at low plasma temperatures. The contribution of neutrals in sputtering is less compared to ions. Roth's equation [11] is used for the chemical yield.

At a target temperature above 900 °C, an enhancement of sublimation has been found by bombardment with light ions at low fluxes [12]. At the divertor conditions, namely, high flux densities and low plasma temperatures, radiation-enhanced sublimation of carbon is expected to be negligible and, therefore, has not been taken into account in the present study. Although the contribution of carbon self-sputtering to erosion increases if $T > 1400$ °C, it will still remain insignificant, because of low impinging particle energy and surface roughness.

3. Calculations of the steady state CFC erosion at glancing angle of incidence

Since the surface temperature of the mock-ups is inhomogeneous due to asymmetrical loading (glancing angle) and asymmetrical cooling (cooling more strong in the centre of monoblock than on the edge), the complicate erosion profile can be achieved. Even more complicated erosion profile can arise in the regimes with dominating chemical erosion mechanism because a dependence of the chemical erosion yield on the surface temperature. The potential temperature and erosion instabilities can occur in the

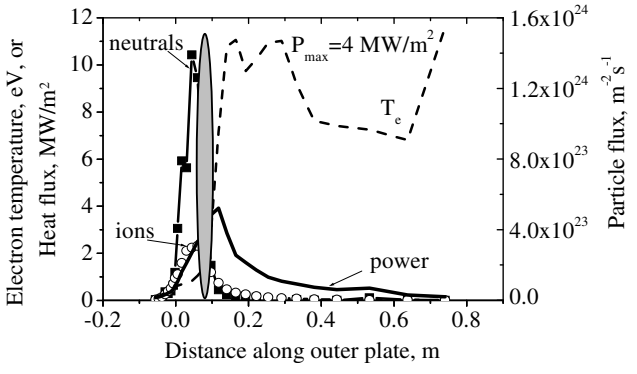

Fig. 1. Profiles of the power density, plasma temperature and particle fluxes along the outer vertical target. Peak power density is 4 MW/m^2. The dark region shows the place with dominating chemical erosion.

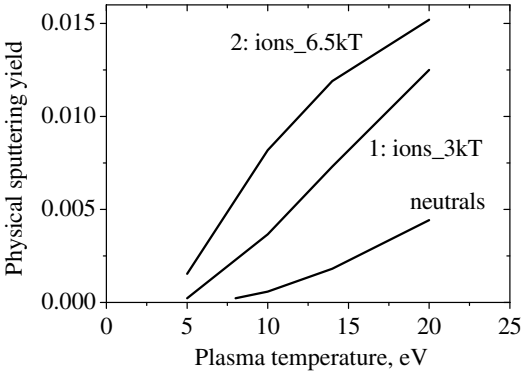

Fig. 2. Physical sputtering yield as a function of the plasma temperature. Curve 1 is for Maxwellian velocity distribution and sheath potential 3 T_e [9] and curve 2 is for Maxwellian velocity distribution and incident ion energy 6.5 T_e [7].

regimes where the chemical erosion considerably contributes to the total erosion. Some cases where the chemical erosion plays a role in the total erosion are presented in Table 1. The power load should be in the range of 3–6 MW/m^2 and ion flux less or equal to 10^{23} D/m^{2}s. Such plasma regimes are expected to occur at the target in a distance of about 0.1 m from the separatrix (Fig. 1).

3.1. Influence of different thermal conductivities of neighbouring monoblocks

Three cases are considered in this paper: case 2 when the physical and chemical yields are similar; case 3 when the physical yield is higher compared to the chemical yield; and case 1 when the physical yield is less compared to the chemical one (Table 1).

The evolution of erosion and temperature profiles with time for the case 2 are shown in Figs. 3 and 4, respectively. The erosion of both monoblocks is the identical for the same thermal conductivities. Both the chemical and physical erosions contribute to the total erosion of mock-ups. The inclined incidence increases both the edge temperature and the edge erosion.

The reduction of the thermal conductivity, λ, of one of the monoblocks increases the surface temperature of this monoblock and may increase or decrease the chemical erosion. Since the chemical erosion yield is an inhomogeneous function of temperature (with a maximum), the cases of an increase or a decrease of the chemical erosion are difficult to predict. The case with a reduction of the chemical erosion of one of the monoblocks by a reduction of the thermal conductivity of this monoblock is shown in Fig. 5. The chemical erosion yield of the first monoblock is comparable with the physical yield and, consequently, gives significant contribution to the erosion: the first monoblock is eroded faster than the second one. The reduction of the chemical yield of the monoblock with reduced thermal conductivity decreases the total erosion of this monoblock (Fig. 6). However, one should not forget about a shadowing effect. A decrease of the erosion of one of the neighbouring monoblocks can result in the deeper edge erosion of the other neighbouring monoblock. Fig. 7 illustrates the erosion of neighbouring monoblocks with different thermal conductivities. The high erosion of the monoblock (b) due to reduced thermal conductivity of this monoblock results in the deeper edge erosion of the less eroded neighbouring monoblock (c). The tendency is obvious: the enhanced erosion of one of the neighbouring monoblocks increases the edge erosion of the less eroded monoblock.

Table 1
Some cases where the chemical erosion contributes to the total erosion on outer vertical divertor target

Case number	Total power density (MW/m^2)	Ion flux normal (D/m^{2}s)	Plasma temperature (eV)
1	4	10^{23}	5
2	4	5×10^{22}	20
3	3.3	7.4×10^{22}	20

Correlation of the ion flux, plasma temperature and power load.

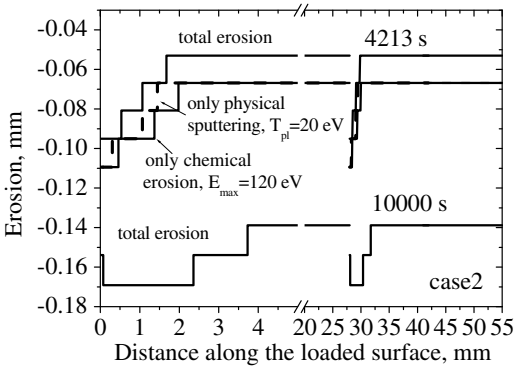

Fig. 3. Erosion profile for the case 2: the power density is 4 MW/m^2, ion flux in respect to the normal to the surface is 5×10^{22} D/m^{2}s, plasma temperature is 20 eV ($E_{max} = 120$ eV). The thermal conductivities of both monoblocks are the same. The contribution of the physical sputtering and chemical erosion is shown for the time = 4213 s.

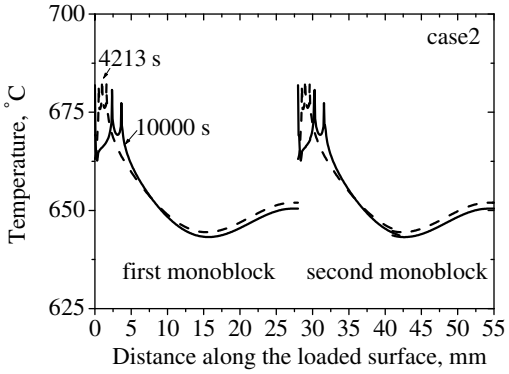

Fig. 4. Surface temperature profile for the case 2: the power density is 4 MW/m^2, ion flux in respect to the normal to the surface is 5×10^{22} D/m^{2}s, plasma temperature is 20 eV ($E_{max} = 120$ eV). The thermal conductivities of both monoblocks are the same.

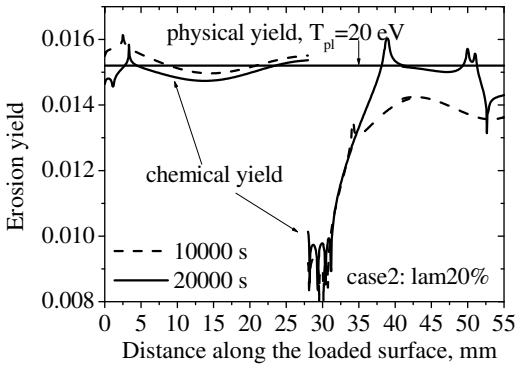

Fig. 5. Chemical and physical yields as a function of the distance along the loaded surfaces for the case 2: the power density is 4 MW/m^2, ion flux in respect to the normal to the surface is 5×10^{22} D/m^{2}s, plasma temperature is 20 eV ($E_{max} = 120$ eV). The thermal conductivity of the second monoblock is 20% less than the first monoblock.

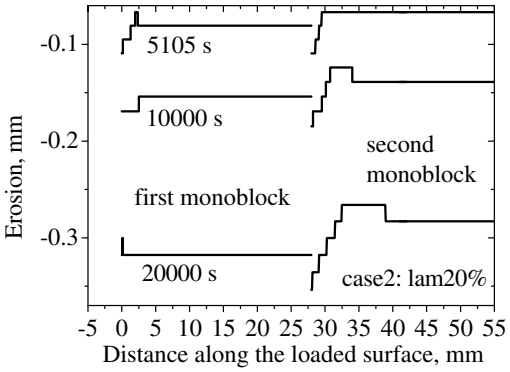

Fig. 6. Erosion profile for the case 2: the power density is 4 MW/m^2, ion flux to the normal in respect to the surface is 5×10^{22} D/m^{2}s, plasma temperature is 20 eV ($E_{max} = 120$ eV). The thermal conductivity of the second monoblock is 20% less than the first monoblock.

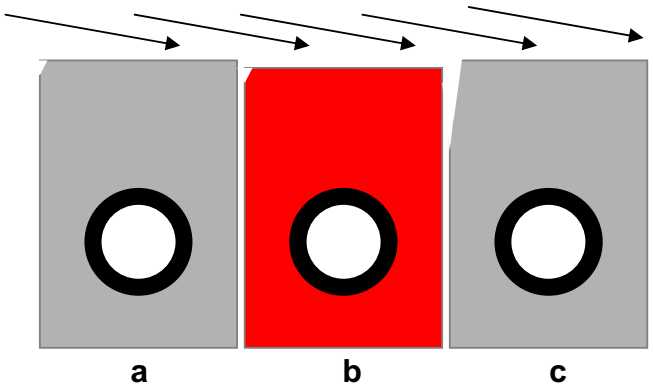

Fig. 7. The different erosion of neighbouring monoblocks due to the different thermal conductivities. The high erosion of the monoblock (b) due to reduced thermal conductivity of this monoblock results in the deeper edge erosion of the less eroded neighbouring monoblock (c).

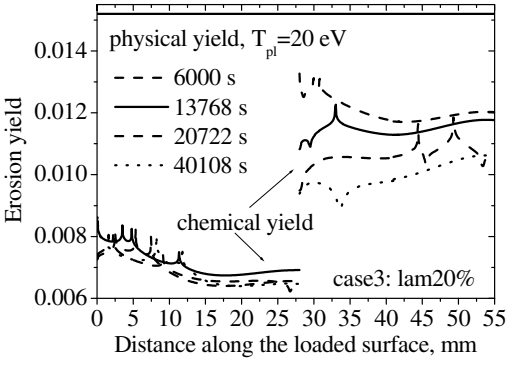

Fig. 8. Chemical and physical yields as a function of the distance along the loaded surfaces for the case 3: the power density is 3.3 MW/m^2, ion flux to the normal in respect to the surface is 7.4×10^{22} D/m^{2}s, plasma temperature is 20 eV ($E_{max} = 120$ eV). The thermal conductivity of the second monoblock is 20% less than the first monoblock.

The reduction of the thermal conductivity, λ, can increase the chemical erosion as it is in the case 3 (Fig. 8). In this case, the second monoblock with reduced λ is eroded faster than the first monoblock (Fig. 9). How-

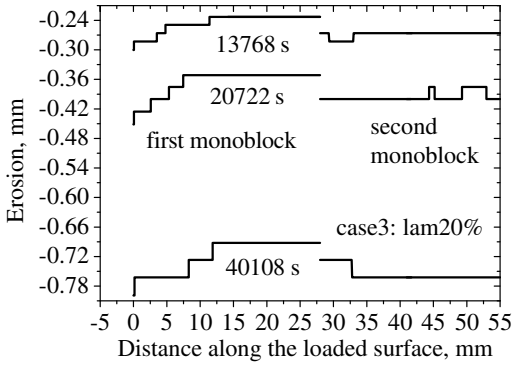

Fig. 9. Erosion profile for the case 3: the power density is 3.3 MW/m^2, ion flux to the normal in respect to the surface is 7.4×10^{22} D/m^{2}s, plasma temperature is 20 eV ($E_{max} = 120$ eV). The thermal conductivity of the second monoblock is 20% less than the first monoblock.

ever, the decreasing of the surface temperature of a monoblock with decreasing of the CFC thickness due to erosion, can reduce the chemical erosion yield. The reduction of the chemical erosion yield with time is shown in Fig. 8. The decrease of the surface temperature of the more eroded monoblock is more pronounced compared to the less eroded monoblock due to less thickness of CFC and better heat removal efficiency. Consequently, the chemical yield of the second monoblock decreases more strongly with time and the difference between temperature and erosion of the two neighbouring components decreases. This means that the temperature/erosion instability can stabilize and the difference between erosion yields of two neighbouring monoblocks will not considerably increase with plasma pulses.

For cold plasma, $T_e = 5$ eV, the chemical erosion is dominated. The chemical yield in the case 1 is higher than the physical one (Fig. 10). The chemical erosion coefficients for both monoblocks do not change significantly with time up to 20 000 s (about 50 discharges). The erosion of the second monoblock with reduced thermal conductivity is less compared to the erosion of the first monoblock with referee

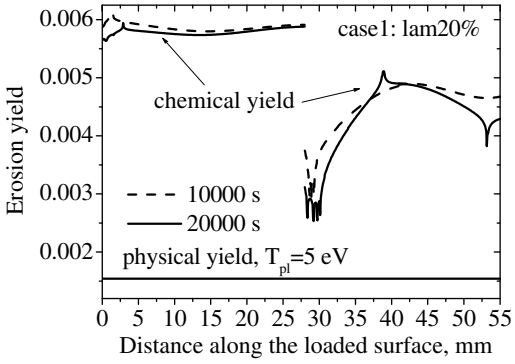

Fig. 10. Chemical and physical yields as a function of the distance along the loaded surfaces for the case 1: the power density is 4 MW/m^2, ion flux to the normal in respect to the surface is 10^{23} D/m^{2}s, plasma temperature is 5 eV ($E_{max} = 30$ eV). The thermal conductivity of the second monoblock is 20% less than the first monoblock.

λ (Fig. 11). The value of the total erosion in the case 1 is less compared to the cases 2 and 3 because of the small energy of incident ions.

From the present results, one can conclude that the difference between erosion of two neighbouring monoblocks can slightly be increased or be decreased with time. In general, this difference does not exceed 20–60 μm for 100 plasma pulses that is about 0.1–0.2% of the total CFC thickness.

Design cyclic thermal loads on the ITER divertor PFCs are 3000 pulses with duration of 400 s at normal operating and 300 slow transient pulses with duration of about 10 s. Because the design number of slow transient pulses is 10% from 3000 normal operating ones, one can assume that each slow transient pulse occurs at each tenth normal operating one. So, typical sequence of design thermal loads is nine normal operating pulses plus one normal operating pulse coupled with one slow transient. Nine pulses correspond about 3600 s. For nine discharges, the difference between erosion of two neighbouring monoblocks with different λ is only about 26 μm.

Effects of ELM's and re-deposition have not been also taken into account although both of them are very important. The re-deposition can change both the chemical and physical yields. ELM's and off-normal events result in high surface temperatures and, thus, prevent the chemical erosion under considered operation conditions. However, if ELM's and off-normal events depress the erosion instability of the two neighbouring components near the separatrix, while they can initiate this instability in the positions further away from the separatrix. In this case, the present analysis should be applied to the monoblocks situated far away from the separatrix. Since the duration of off-normal events is much less than the duration of normal operation discharge, a significant difference in the erosion of neighbouring components is not expected. In general, the erosion arising from transient power and particle pulses is potentially of more concern than steady state erosion. However, the aim of this study is not to find the absolute value of erosion but to investigate if the difference in the erosion of two neighbouring components will increase with the plasma pulses or it will be more or less stable and does not results in unacceptable erosion of one of the components.

3.2. Influence of defects between CFC armour and CuCrZr cooling tube

For the carbon armour joints, the bore of the CFC monoblocks are lined with a pure Cu layer cast onto a laser-textured and Ti-metallised surface, so-called active metal casting (AMC). The Cu in the bore of the monoblocks is machined to size prior to them being low temperature (~500 °C) hot-isostatically pressed (HIP) to a CuCrZr tube. The precipitation hardened CuCrZr alloy has been selected over other Cu alloys because of its good postirradiation fracture toughness. In fact, several techniques might be used for making the Cu–CuCrZr joint (furnace braze with fast quench, rapid brazing using ohmic or inductive heating, or HIP-ing), but the HIP process gives optimised mechanical and thermal properties, and minimises the residual strains in the critical Cu–CFC joint. In any way, the defects can not be avoidable during the fabrication. Defects are defined by their location, θ, and their extension, $\Delta\theta$, as it is shown in Fig. 12. The conductivity of the elements around the copper tube can be modified using a dummy material in order to simulate a partial detachment between the cooling channel and the CFC corresponding to the defect position.

The defects of the size of $\Delta\theta = 60°$ and $\Delta\theta = 90°$ with position of the centre of the defect of $\theta = -30°$ or $\theta = -45°$ (left defects) and with positions of $\theta = 30°$ or $\theta = 45°$ (right defects) have been considered.

A partial loss of the thermal contact between the CFC and cooling tube due to a defect results in a local increase of the surface temperature. In the presence of the left situated defect, the temperature on the left side of the loaded surface is increased, while in the presence of the right situated defects, the temperature on the right side of the loaded

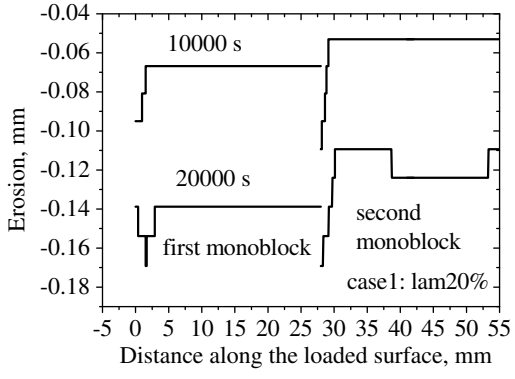

Fig. 11. Erosion profile for the case 1: the power density is 4 MW/m^2, ion flux to the normal in respect to the surface is 10^{23} D/m^{2}s, plasma temperature is 5 eV ($E_{max} = 30$ eV). The thermal conductivity of the second monoblock is 20% less than the first monoblock.

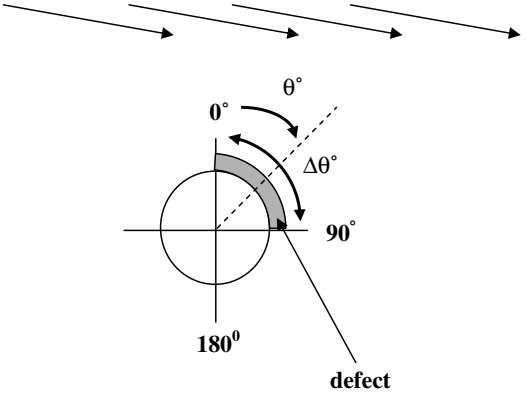

Fig. 12. A location, θ, and an extension, $\Delta\theta$, of a defect between CFC and cooling tube. For example, the size of the present defect is $\Delta\theta = 90°$ and the position is $\theta = 45°$.

surface is increased. The right situated defects have less influence on erosion compared to the left situated defects because particles are coming at glancing angle from the left side in the present design as shown in Fig. 12.

An increase of the erosion in the presence of a left defect ($\Delta\theta = 90°$ and $\theta = -30°$) in the first monoblock is shown in Fig. 13 for the case 3. The erosion yields are shown in Fig. 14. The presence of a left defect increases the chemical erosion coefficient (by increasing the surface temperature) and, consequently, increases the contribution of the chemical erosion to the total erosion. So, the first monoblock is eroded faster compared to the second one. However, a reduction of the thermal conductivity of a monoblock results in a significant increase of the surface temperature along those loaded surface of the component while the local detachment of the thermal contact between the CFC and cooling channel has less influence on an increase of the surface temperature. Consequently, the influence of a defect in one of the neighbouring monoblocks on erosion/temperature instability is less pronounced compared to the difference in thermal conductivities of neighbouring monoblocks. Moreover, there is not an effect of deeper edge erosion of less eroded monoblock in the presence of a defect as it is in the case of different thermal conductivities. Fig. 15 illustrates the different erosion of neighbouring monoblocks due to a presence of a defect in one of the monoblocks. The erosion of the monoblock (b) with a defect between the CFC and the cooling tube is higher compared to neighbouring monoblocks (a) and (c) because of higher chemical erosion yield.

Finally, one example where there is a defect in the first monoblock and the second monoblock has a reduced thermal conductivity has been considered. No strong difference in the erosion of monoblocks has been observed (Fig. 16). The presence of a defect in the first monoblock results in a higher erosion of this monoblock compared to the case without a defect. The defect in the first monoblock can prevent the edge erosion of this monoblock caused by the erosion of the second monoblock with reduced thermal conductivity. Thus, a combination of one monoblock with a defect and another one with reduced thermal conductivity can, in some cases, even reduce the variation in the

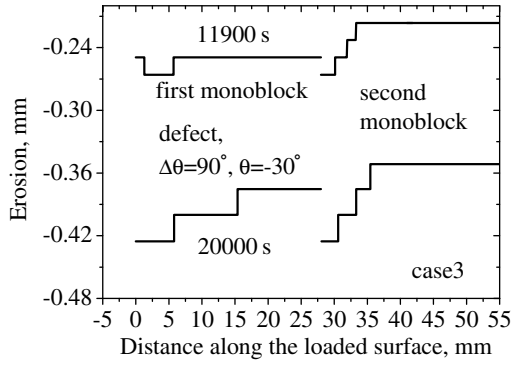

Fig. 13. Erosion profile for the case 3. The power density is 3.3 MW/m^2, ion flux to the normal in respect to the surface is 7.4×10^{22} D/m^{2}s, plasma temperature is 20 eV ($E_{max} = 120$ eV). There is a left defect between the CFC and the cooling tube of a size of $\Delta\theta = 90°$ and a position of $\theta = -30°$ in the first monoblock. There are no defects in the second monoblock.

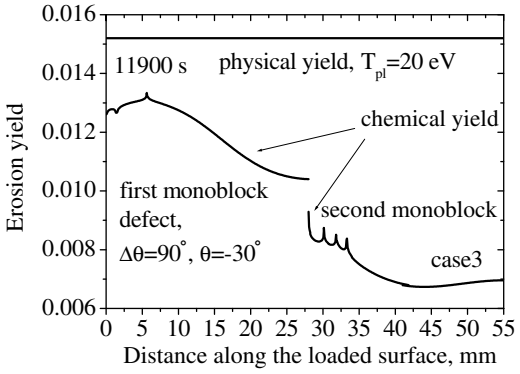

Fig. 14. Erosion yields for the case 3. The power density is 3.3 MW/m^2, ion flux to the normal in respect to the surface is 7.4×10^{22} D/m^{2}s, plasma temperature is 20 eV ($E_{max} = 120$ eV). There is a left defect between the CFC and the cooling tube of a size of $\Delta\theta = 90°$ and a position of $\theta = -30°$ in the first monoblock. There are no defects in the second monoblock.

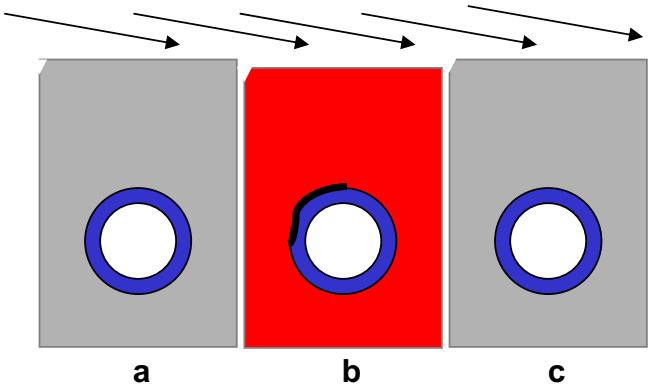

Fig. 15. The different erosion of neighbouring monoblocks due to a presence of a defect between the CFC and the cooling tube in one of the monoblocks.

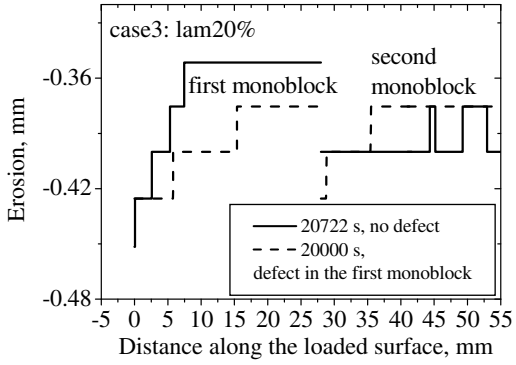

Fig. 16. Erosion profile for the case 3. The power density is 3.3 MW/m^2, ion flux to the normal in respect to the surface is 7.4×10^{22} D/m^{2}s, plasma temperature is 20 eV ($E_{max} = 120$ eV). Solid lines are for monoblocks without any defects. Dashed lines are for a presence of a left defect between the CFC and the cooling tube (size of $\Delta\theta = 90°$ and a position of $\theta = -30°$) in the first monoblock. The thermal conductivity of the second monoblock is 20% less than the first monoblock for both cases.

erosion of neighbouring components. At least, there is no indication of higher edge erosion of one of the monoblocks compared to another one.

4. Conclusions

The paper presents the investigation of the difference in temperature distributions and erosion profiles of the two neighbouring divertor components with variation of thermal conductivity and/or assembly defects between CFC armour and CuCrZr cooling tube. This difference or erosion/temperature instability takes place in the special operation regimes where the chemical erosion dominates, namely near the separatrix.

The variation in the thermal conductivity of two neighbouring monoblocks by 20% does not exceed the difference in the erosion in 20–60 μm that is about 0.1–0.2% of the total CFC thickness. This difference in the erosion of two neighbouring monoblocks can slightly be increased or be decreased with plasma pulses but it is not a critical point even without taking into account the off-normal events. The calculations have been done up to 50 plasma discharges without taking into account ELMs, transient and disruptions which, probably, will depress the chemical erosion by a significant increase of the surface temperature and, consequently, depress the instability. On the other hand, off-normal events can initiate this instability in the positions further away from the separatrix. In this case, the present analysis would be also valid for the monoblocks situated far away from the separatrix. However, since the duration of off-normal events is much less than the duration of normal operation discharge, the difference in the erosion of neighbouring components is expected to be negligible.

The influence of a defect in the joint area between CFC and cooling tube with a maximum available size of 90° in circumferential direction from the apex on erosion and temperature instabilities is less pronounced compared to the difference in thermal conductivities of neighbouring monoblocks.

Effect of deeper edge erosion of less eroded monoblock has been observed. Such effect takes place only in the case of different thermal conductivities of two neighbouring monoblocks.

According to the preliminary results, a defect in the joint area between CFC armour and cooling tube of a size of 90° and a reduction of the thermal conductivity by 20% of one of the neighbouring monoblocks are acceptable with point of view of erosion instability for the present design and operation conditions. The effect of ELM's and off-normal events as well as re-deposition and neutron irradiation could be taking into account for the future investigation.

Acknowledgement

This work, supported by the European Communities under the European Contract 05/1248 of Association between EURATOM and CEA, was carried out within the framework of the European Fusion Development Agreement. The views and opinions expressed herein do not necessarily reflect those of the European Commission.

References

[1] G. Janeschitz, in: 14th PSI, Plasma Surface Interaction Conference, Rosenheim, May 2000.
[2] M. Rödig, R. Duwe, W. Kuhnlein, J. Linke, M. Scheerer, I. Smid, B. Wiechers, J. Nucl. Mater. 258–263 (1998) 967.
[3] G. Federici, J.N. Brooks, D.P. Coster, G. Janeschitz, A. Kukuskhin, A. Loarte, H.D. Pacher, J. Stober, C.H. Wu, J. Nucl. Mater. 290–293 (2001) 260.
[4] E. D'Agata, O.V. Ogorodnikova, R. Tivey, C. Lowry, J. Schlosser, Fusion Eng. Des. 82 (2007) 1739.
[5] O.V. Ogorodnikova, Influence of the carbon erosion on the acceptance criteria of the ITER divertor, CEA report CFP/NTT-2007.004 (DRFC/SIPP), 2007.
[6] P.C. Stangeby, G.M. McCracken, Nucl. Fusion 30 (1990) 1225.
[7] W. Eckstein, unpublished data.
[8] A. Kukushkin, private communication.
[9] W. Eckstein, Calculated sputtering, reflection and range values, IPP 9/132 (2002).
[10] A. Kirschner, D. Borodin, S. Droste, V. Philipps, U. Samm, G. Federici, A. Kukushkin, A. Loarte, J. Nucl. Mater. 363–365 (2007) 91260.
[11] J. Roth et al., J. Nucl. Mater. 337–339 (2005) 970.
[12] C.H. Wu, J. Nucl. Mater. 145–147 (1987) 448.